

Nanowarriors from Mentha: Unleashing Nature's Antimicrobial Arsenal with Cerium Oxide Nanoparticles

Maarij Khan, Rahmat Wali, Zia-ur-Rehman Mashwani,* Naveed Iqbal Raja, Riaz Ullah, Ahmed Bari, Shah Zaman, and Sohail*



Cite This: *ACS Omega* 2024, 9, 15449–15462



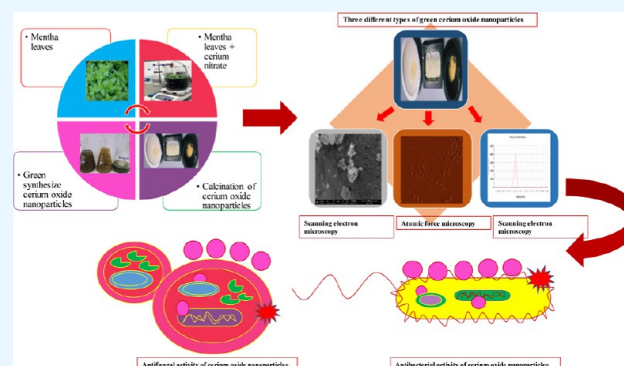
Read Online

ACCESS |

Metrics & More

Article Recommendations

ABSTRACT: Medicinal plant-based cerium oxide nanoparticles (CeO_2NPs) possessed excellent antimicrobial properties against multiple strains of Gram-positive and Gram-negative bacteria. The CeO_2NPs are popular because their electropositive charged surface causes oxidation of plasma membrane and facilitates the penetration of CeO_2NPs inside the pathogen body. In the present research work, CeO_2NPs stabilized with *Mentha* leaf extract; as a result, nanoparticles surface-bonded with various functional groups of phytochemicals which enhanced the therapeutic potential of CeO_2NPs . The inhibition percentage of CeO_2NPs was evaluated against eight pathogenic Gram-positive bacteria *Staphylococcus aureus* and *Streptococcus epidermidis*; Gram-negative bacteria *Escherichia coli*, *Stenotrophomonas maltophilia*, *Comamonas* sp., *Halobacterium* sp., and *Klebsiella pneumoniae*; and plant bacteria *Xanthomonas* sp. The antifungal properties of CeO_2NPs were evaluated against three pathogenic fungal species *Bipolaris sorokiniana*, *Aspergillus flavus*, and *Fusarium oxysporum* via the streak plate method. The antimicrobial inhibitory activity of CeO_2NPs was good to excellent. The current research work clearly shows that three different medicinal plants *Mentha royleana*, *Mentha longifolia*, and *Mentha arvensis* based CeO_2NPs , variation in nanoparticle sizes, and surface-to-volume ratio of green CeO_2NPs are three factors responsible to generate and provoke antimicrobial activities of CeO_2NPs against human pathogenic bacteria and plant infecting fungi. The results show that CeO_2NPs possessed good antimicrobial properties and are effective to use for pharmaceutical applications and as a food preservative because of low toxicity, organic coating, and acceptable antimicrobial properties. This study showed a rapid and well-organized method to prepare stable phytochemical-coated CeO_2NPs with three different plants *M. royleana*, *M. longifolia*, and *M. arvensis* with remarkable antibacterial and antifungal characteristics.



1. INTRODUCTION

Nanotechnology is an emerging area of science. Nanoparticles have wide applications in agriculture, cosmetics, medicines, and food industry. Nanoparticles are popular moieties because of their unique size-to-volume ratio. Recently, different size, shape, and metallic nature nanoparticles are available. Cerium is a rare-earth element belonging to lanthanide. Cerium is distinctive because of variable oxidation states Ce^{4+} to Ce^{3+} . Cerium rapidly binds free radical species and changes their oxidation state Ce^{4+} to Ce^{3+} . There are three popular methods used to synthesize nanoparticles: (1) chemical method, (2) physical method, and (3) biological method. The physical and chemical methods are expensive, require costly chemicals and special laboratory equipment, and are toxic to living things. The biological method to synthesize nanoparticles is cost-effective, does not require special equipment, and can be practiced easily. In the biological method, the reducing agent can be prepared from algae, fungi, bacteria, and plants, and biological derivatives can be used as a reducing agent, but all

other biological materials had accessibility issues, were treated under special laboratory conditions, were difficult to handle, and required extra precautions for culturing and extraction. The plant-based synthesis of nanoparticles is an advantageous method because it is (1) cost-effective and (2) easy to handle, (3) requires less-controlled conditions, (4) shows less chemotoxicity, (5) is biodegradable, (6) has organic nature, (7) is highly stable in solution, and (8) is less reactive in different solutions.²⁶ In the given study, plant-based synthesis of nanoparticles was used to prepare CeO_2NPs using three species of genus *Mentha*. In the present research study, the

Received: January 8, 2024
Revised: February 24, 2024
Accepted: February 28, 2024
Published: March 22, 2024



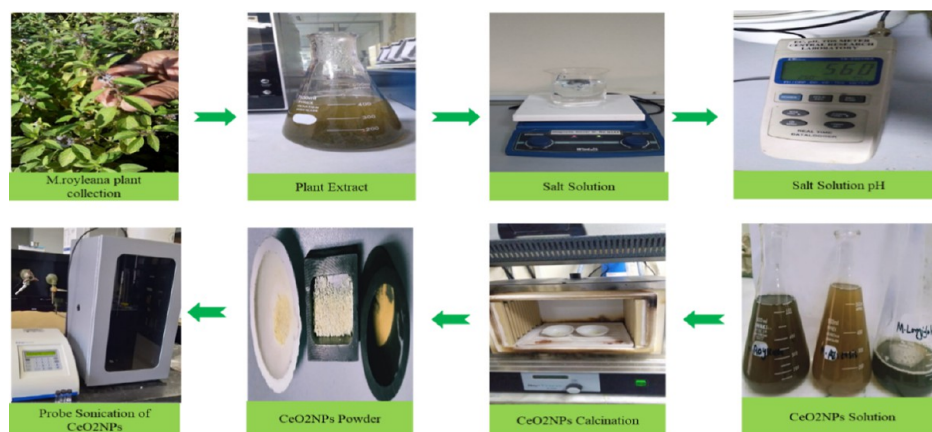


Figure 1. Figurative representation of green synthesis of CeO₂NPs. The preparation of Mentha leaf extract, mixing of cerium nitrate hexahydrate salt and leaf extract, separation of CeO₂NPs through centrifugation, calcination of oven-dried CeO₂NPs, and probe sonication of CeO₂NPs before biological applications.

three plant species from genus *Mentha* belonging to family Lamiaceae were used.

Mentha is a genus that contains many aromatic and medicinal species used in the treatment of various ailments for thousands of years. *Mentha* possesses special importance in the history of medicine, and many researches are available for the utilization of *Mentha* extract for antimicrobial purposes.²⁴ *Mentha* is a rich source of essential oils (piperitone, pulegone, cis-piperitone epoxide, menthol, menthone, and carvone) and phytochemicals (caffeic acid, gallic acid, ferulic acid, oleanolic acid, menthyl acetate, linalool, and linalyl acetate).^{24,28} *Mentha* is a big bank of highly important phytochemicals, essential oils, antioxidants, antimicrobial agents, and anticancer compounds.²⁸ In addition, cerium is a rare-earth metal with variable oxidation state, and the electropositive nature rapidly initiates lipid peroxidation when comes in contact with the cell wall and plasma membrane.²⁵ Using the available information in the literature, we combined phytochemical and metal ore characteristics, synthesized green CeO₂NPs, and tested against pathogenic bacterial strains and fungal species.

For the formation of green CeO₂NPs, the leaf extract of *Mentha longifolia*, *Mentha arvensis*, and *Mentha royleana* was used as a reducing agent, which makes CeO₂NPs highly biocompatible and biodegradable for biological systems. Three basic steps are involved: (1) cerium nitrate hexahydrate salt ionization in Millipore water, (2) the reduction of the ionized cerium with *Mentha* leaf extract, and at this point, cerium (Ce) separates from nitrate NO₃, and (3) coating of CeO₂NPs with the secondary metabolites of the *Mentha* leaf extract. Three mint species *M. longifolia*, *M. arvensis*, and *M. royleana* were collected from different areas of Pakistan. Mint is a big source of essential oils and secondary metabolites, and ancient people utilized mint for the treatment of many diseases. In the present research, CeO₂NPs were synthesized using the leaf extract of three *Mentha* species.¹¹ Nanoparticles are extensively in use for the medication of infectious diseases that arise due to drug-resistant pathogens. In the last two decades, nanoparticles have gained the attention of researchers for their wide range of applications in biomedical field due to possession of unique physical and chemical properties.^{9,10} Among all nanoparticles, CeO₂NPs exhibit promising antibacterial and antifungal activities.

CeO₂NPs gain attention because of their reactive oxygen species (ROS) scavenging/quenching potential.^{12,13}

In the last two decades, the drug resistance of microorganisms and the transmission of infection have become a global challenge.¹ Multidrug-resistant bacteria possess the capacity to escape or run away from the killing of antibiotics.² Pathogenic microorganisms are responsible for causing minor skin infections to major fatal diseases in humans, such as pneumonia, meningitis, surgical infection, septicemia, and endocarditis.³ Over time, different antibiotics were used against pathogenic bacteria; eventually, a large number of bacteria gained resistance against many antibiotics; there are many factors involved behind the issue, such as consumption of a combination of antibiotics, the resistant gene present in the genetic material becomes dominant, without screening bacterial species, multiple antibiotics were suggested by the doctors, a combination of antibiotics causes killing of nonresistant bacterial species and resistant bacterial species left in the body process infection, and these species have the capacity of completion; hence, resistant species are naturally selected.^{4,5} Undoubtedly, reports also revealed that the capabilities of multidrug-resistant pathogens are critically harmful for immunocompromised patients that are hospitalized for other chronic diseases like, diabetes mellitus, chronic lung infection, cardiovascular disease, cancer, and obstructive pulmonary diseases.⁶ Patients with chronic diseases may be susceptible to wounds and challenging to heal despite intensive treatments. The multidrug resistance of bacteria is responsible to cause instability and emergency in healthcare departments and shifting affordable treatments to large and expensive treatment processes. In consequence, the world needs new antibiotics for resistance species of bacteria. In a recent research work, eight bacterial strains were treated with three different green synthesized CeO₂NPs: Gram-negative bacterial strains (*Stenotrophomonas maltophilia*, *Xanthomonas oryzae*, *Comamonas* sp., *Halobacterium* spp., *Escherichia coli*, and *Klebsiella pneumoniae*) and Gram-positive bacterial strains (*Staphylococcus aureus* and *Staphylococcus epidermidis*).¹⁴

Fungi are living organisms placed in separate Kingdom fungi. Fungi infect humans, animals, and plants equally and extensively spread mycelia at long distances. Resistant fungal species have become a public health problem in the constantly changing world. Fungal species largely cause skin mycosis,

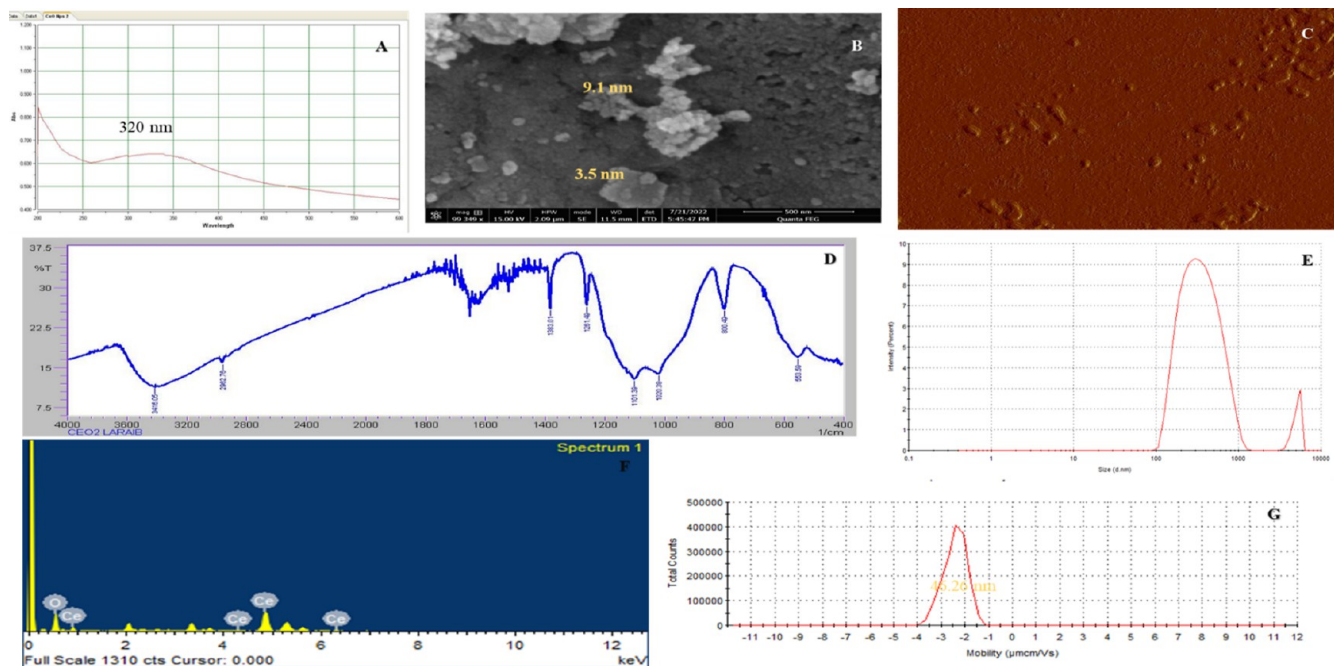


Figure 2. (A) UV–visible spectroscopy results of green synthesized $\text{CeO}_2\text{NPs}^{\text{MA}}$; (B) SEM micrograph of green synthesized $\text{CeO}_2\text{NPs}^{\text{MA}}$; (C) AFM micrographs of $\text{CeO}_2\text{NPs}^{\text{MA}}$; (D) FTIR spectrum confirms the localization of phytochemicals at the surface of green synthesized $\text{CeO}_2\text{NPs}^{\text{MA}}$, spectral peaks/bands at 470.65, 802.41, 860.28, 1028.09, 1103.32, 1261.41, 1384.94, 1554.58, and 3404.47, halo group/amine, alkane, alkene, anhydride, aliphatic, alkyl–aryl–ether, phenol, alpha-beta-unsaturated ketone, and alkyl group were observed at the CeO_2NP surface. (D) $\text{CeO}_2\text{NPs}^{\text{MA}}$; (E) DLS graphical representation of $\text{CeO}_2\text{NPs}^{\text{MA}}$; (F) EDX confirmed the presence of $\text{CeO}_2\text{NPs}^{\text{MA}}$; and (G) zeta potential graphical representation expresses positive charge at $\text{CeO}_2\text{NPs}^{\text{MA}}$. $\text{CeO}_2\text{NPs}^{\text{MA}}$ were prepared by using three different genus *Mentha* leaf extracts.

urinary tract infection, reproductive tract infection, and bladder infection in humans. Fungal infection is life-threatening for immunocompromised hospitalized patients. The long treatment duration and frequent use of prophylactic agents facilitate the emergence of resistant fungal species.^{7,8} Even resistance often seems to be against different antifungal agents like itraconazole, fluconazole, and voriconazole in the hospital environment.⁸ Fungal pathogens severely damage seeds crops, oil seed crops, nuts, dry fruits, and fleshy fruits. Fungi produce a large number of spores spread through wind, transfer of contaminated soils in the fields, using contaminated harvesting tools, and water splash. The fungal pathogens not only destroy field crops but also contaminate storage seeds such as wheat, corn, rice, and canola. In present study, three fungal species *Aspergillus flavus*, *Fusarium oxysporum*, and *Bipolaris sorokiniana* were treated with three different green synthesized CeO_2NPs , and popular antifungal drug fluconazole was used as the positive control.

2. MATERIALS AND METHODOLOGY

2.1. Collection of the Plant Material. Plant extracts for use as reducing agents were prepared from three distinct species within genus *Mentha*. *M. royleana* L. was collected from the Upper Dir District in Malakand Division of province Khyber Pakhtunkhwa, Pakistan. *M. royleana* L. specimens were collected in Upper Dir, a district in the Malakand Division of Khyber Pakhtunkhwa province, Pakistan. *M. longifolia* L. samples were collected from Quaid-i-Azam University in Islamabad, Pakistan. *M. arvensis* L. specimens were collected at Pir Mehr Ali Shah Arid Agriculture University in Rawalpindi, Punjab province, Pakistan. The collected plant specimens were dried and then mounted on herbarium sheets. Voucher

specimens were duly submitted to the herbarium at Pir Mehr Ali Shah Arid Agriculture University in Rawalpindi.

2.1.1. Preparation of the Plant Material. The plant material was washed with tap water to remove soil and other organic matter. It was washed with distilled water two to three times. Leaves were separated from the branches and placed in shade for 10 days. The dried plant leaves were ground into a powder. The powder was stored in an airtight container and kept in a refrigerator for further use.¹¹

2.1.2. Preparation of the Plant Extract. For leaf extract preparation, 10 g of powder was weighed in a 200 mL glass beaker, dissolved in 120 mL of distilled water, and placed on a hot plate for 2 h at 80 °C. The plant extract was filtered three times using Whatman filter paper. The pure extract (free from organic particles) was stored in a refrigerator at 4–5 °C for further use.¹¹

2.1.3. Green Synthesis of CeO_2NPs . About 0.04 g of salt of $\text{Ce}(\text{NO}_3)_3 \cdot 6\text{H}_2\text{O}$ was dissolved in 400 mL of deionized water, and the solution was placed on a hot plate for 40 min at 150 °C. Then, 75 mL of plant extract was added into the salt solution dropwise. The solution was placed on a hot plate for 6 h. CeO_2NP synthesis was confirmed through a white precipitate in solution. The hot plate was turned off, and the solution was left overnight. The solution was again placed on a hot plate for 2 h. At last, the CeO_2NP solution was centrifuged and washed 5× with concentrated methanol (to remove the extra organic material). CeO_2NPs were oven-dried at 64 °C for 24 h (Figure 1). Finally, CeO_2NPs were kept in a muffle furnace for at 400 °C for 2 h.¹¹

2.1.4. Chemical Stability of CeO_2NPs . The CeO_2NP solution with pH 5.6 and the CeO_2NP electrostatic attraction and coating of CeO_2NPs with phytochemical functional groups certify by FTIR spectrum results that the localization

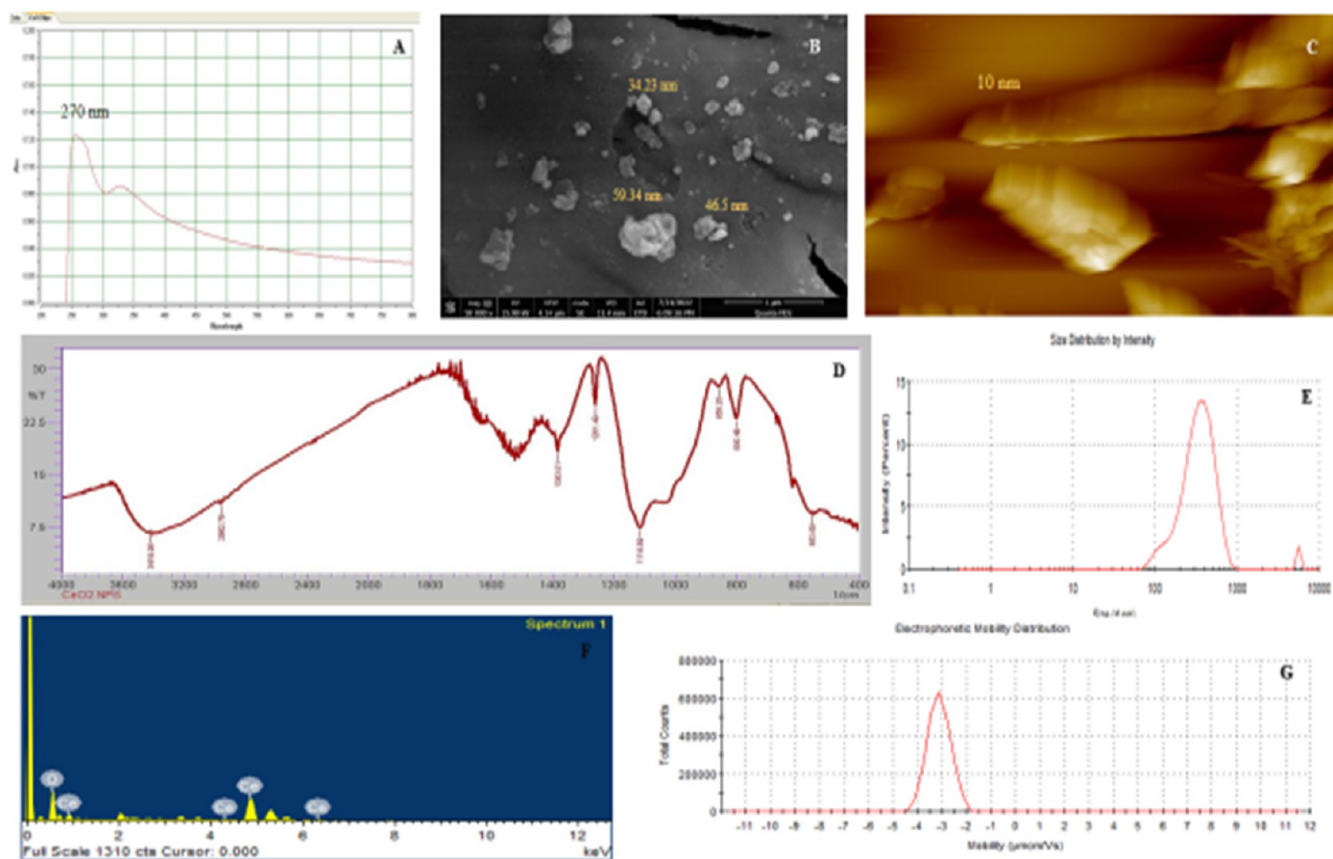


Figure 3. (A) UV–visible spectroscopy results of green synthesized $\text{CeO}_2\text{NPs}^{\text{ML}}$; (B) SEM micrograph of green synthesized $\text{CeO}_2\text{NPs}^{\text{ML}}$; (C) AFM micrographs of $\text{CeO}_2\text{NPs}^{\text{ML}}$; (D) FTIR spectrum confirm the localization of phytochemicals at the surface of green synthesized $\text{CeO}_2\text{NPs}^{\text{ML}}$, spectral peaks/bands at 470.65, 802.41, 860.28, 1028.09, 1103.32, 1261.41, 1384.94, 1554.58, and 3404.47; halo group/amine, alkane, alkene, anhydride, aliphatic, alkyl–aryl–ether, phenol, alpha–beta-unsaturated ketone, and alkyl group were observed at the CeO_2NP surface. (D) $\text{CeO}_2\text{NPs}^{\text{ML}}$; (E) DLS graphical representation of $\text{CeO}_2\text{NPs}^{\text{ML}}$; (F) EDX confirmed the presence of $\text{CeO}_2\text{NPs}^{\text{ML}}$; (G) zeta potential graphical representation of $\text{CeO}_2\text{NPs}^{\text{ML}}$ expresses positive charge at $\text{CeO}_2\text{NPs}^{\text{ML}}$. $\text{CeO}_2\text{NPs}^{\text{ML}}$ were prepared by using three different genus *Mentha* leaf extracts.

of phytochemicals at the surface of green synthesized CeO_2NPs ; spectral peaks/bands at 470.65, 802.41, 860.28, 1028.09, 1103.32, 1261.41, 1384.94, 1554.58, and 3404.47 cm^{-1} , and peak number indicate the presence of chemical groups including halo group/amine, alkane, alkene, anhydride, aliphatic, alkyl–aryl–ether, phenol, alpha–beta-unsaturated ketone, and alkyl group at the CeO_2NP surface (<https://www.sigmaaldrich.com/PK/en/technical-documents/technical-article/analytical-chemistry/photometry-and-reflectometry/ir-spectrum-table>). Additionally, phytochemical coating provides hydrophilicity and supports the solubility and stability of CeO_2NPs in water and buffer. The organic coating stabilizing feature facilitates the formation of electrostatic and protective layers that protect nanoparticle aggregation and crystal formation. The organic coating enhanced CeO_2NPs ' utility in drug delivery systems, and water-soluble dispersion stabilizes during oral bioavailability and reduces biological reactions.^{11,29}

2.2. Characterization Techniques for CeO_2NPs . UV–visible spectroscopy was performed to examine the absorbed and transmitted light through an analytical sample, which confirms the quantity of suspended particles in solution (Labomed UVD 3500, Los Angeles, CA, USA). Scanning electron microscopy was performed to evaluate the size and shape of CeO_2NPs along with topographical feature (SIGMA

model (MIRA3; TESCAN Brno)) at the Institute of Space Technology, Islamabad, Pakistan. Energy-dispersive X-ray spectroscopy was performed to diagnose the chemical/elemental composition of CeO_2NPs (JSM-IT 500 Jeol, Boston, MA, USA) at the Institute of Space Technology, Islamabad, Pakistan. Fourier transform infrared spectroscopy identifies the presence of functional groups at the surface of green synthesized CeO_2NPs (PerkinElmer FTIR-Spectrum, Akron, OH, USA) at the Institute of Space Technology Islamabad, Pakistan. Dynamic light scattering is a new technique used to determine the homogeneity of the analyzing material in the solution (Malvern Zetasizer Nano-ZS ZEN 3600) at the University of Texas at Austin, USA. Zeta potential is related to confirm the net charge on the surface of CeO_2NPs (Malvern Zetasizer Nano-ZS ZEN 3600), University of Texas at Austin, USA. Atomic force microscopy was performed to measure the size and shape of CeO_2NPs which are less than 30 nm (Park NX 10 USA) at the University of Texas at Austin, USA.^{11,27}

2.3. Antibacterial Assay. The antibacterial assay for green synthesized CeO_2NPs was accomplished through the agar well diffusion for eight bacterial strains. Gram-positive (*S. aureus* and *S. epidermidis*), Gram-negative (*E. coli*, *S. maltophilia*, *Comamonas* sp., *Halobacterium* sp., and *K. pneumoniae*), and plant bacterial (*Xanthomonas* sp.) colonies

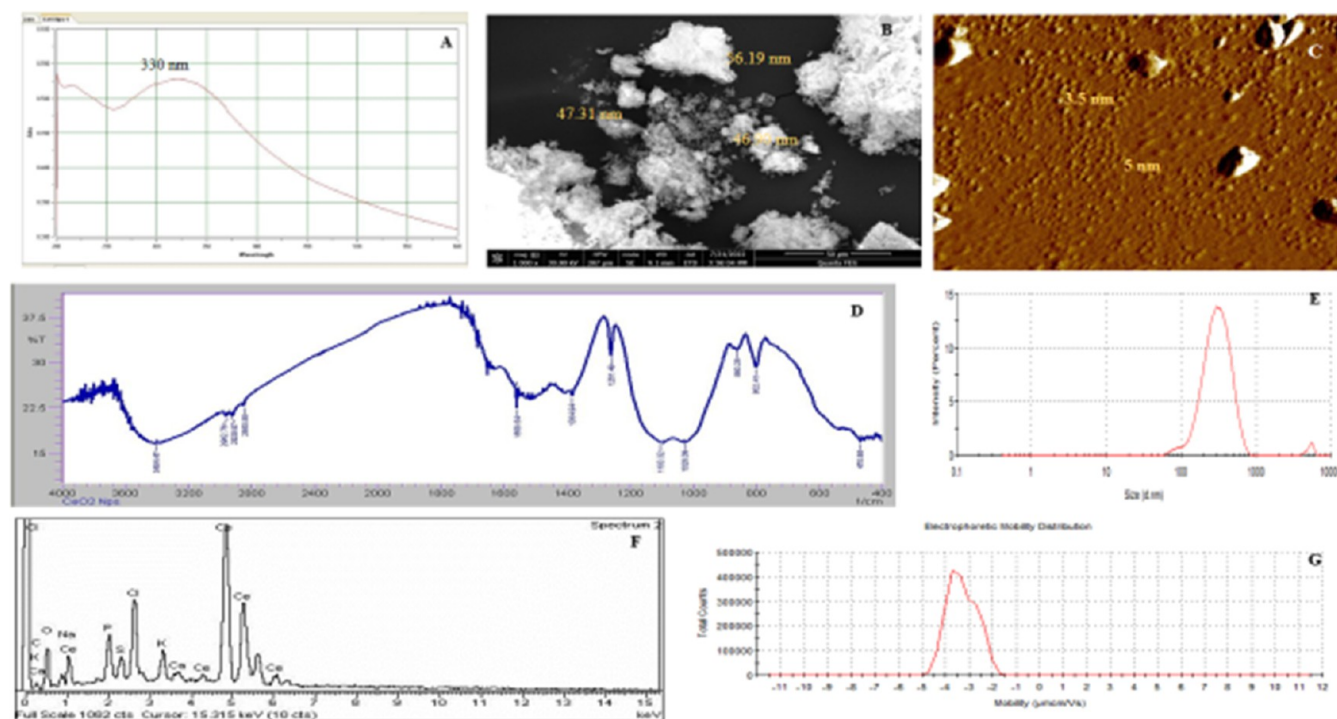


Figure 4. (A) UV–visible spectroscopy results of green synthesized $\text{CeO}_2\text{NPs}^{\text{M.R}}$; (B) SEM micrograph of green synthesized $\text{CeO}_2\text{NPs}^{\text{M.R}}$; (C) AFM micrographs of $\text{CeO}_2\text{NPs}^{\text{M.R}}$; (D) FTIR spectrum confirms the localization of phytochemicals at the surface of green synthesized $\text{CeO}_2\text{NPs}^{\text{M.R}}$; spectral peaks/bands at 470.65, 802.41, 860.28, 1028.09, 1103.32, 1261.41, 1384.94, 1554.58, and 3404.47; and halo group/amine, alkane, alkene, anhydride, aliphatic, alkyl–aryl–ether, phenol, α – β -unsaturated ketone, and alkyl group were observed at the $\text{CeO}_2\text{NPs}^{\text{M.R}}$ surface. (D) $\text{CeO}_2\text{NPs}^{\text{M.R}}$; (E) DLS graphical representation of $\text{CeO}_2\text{NPs}^{\text{M.R}}$; (F) EDX confirmed the presence of $\text{CeO}_2\text{NPs}^{\text{M.R}}$; and (G) zeta potential graphical representation of $\text{CeO}_2\text{NPs}^{\text{M.R}}$ express positive charge at $\text{CeO}_2\text{NPs}^{\text{M.R}}$. $\text{CeO}_2\text{NPs}^{\text{M.R}}$ were prepared by using three different genus *Mentha* leaf extracts.

Table 1. Coding and Doses of CeO_2NPs Used in the Research Study^a

| sr. no. | treatments $\text{CeO}_2\text{NPs}^{\text{M.A}}$ ($\mu\text{g}/\text{mL}$) | treatments $\text{CeO}_2\text{NPs}^{\text{M.L}}$ | treatments $\text{CeO}_2\text{NPs}^{\text{M.R}}$ ($\mu\text{g}/\text{mL}$) |
|---------|--|--|--|
| 1 | 62.5 | 62.5 $\mu\text{g}/\text{mL}$ | 62.5 |
| 2 | 125 | 125 $\mu\text{g}/\text{mL}$ | 125 |
| 3 | 250 | 250 $\mu\text{g}/\text{mL}$ | 250 |
| 4 | 500 | 500 $\mu\text{g}/\text{mL}$ | 500 |
| 5 | 1000 | 1000 $\mu\text{g}/\text{mL}$ | 1000 |

^a $\text{CeO}_2\text{NPs}^{\text{M.A}}$. (*M. arvensis* based cerium oxide nanoparticles). $\text{CeO}_2\text{NPs}^{\text{M.L}}$. (*M. longifolia* based cerium oxide nanoparticles). $\text{CeO}_2\text{NPs}^{\text{M.R}}$. (*M. royleana* based cerium oxide nanoparticles).

were cultured in a nutrient broth at 37 °C in an incubator shaker for 72 h. The Mueller Hinton agar was sterile in an autoclave for 3 h at 115 °C HICLAVE HVE Model HVE-50 (HIRAYAMA Manufacturing Corp.). Subsequently, 34 g of nutrient agar was dissolved in 1 L of deionized water, and 15 mL of agar was poured into each Petri plate; after cooling and solidification, it was inoculated with a bacterial culture and left for 24 h. The colony forming unit was 7×10^5 . The bacterial cell culture dilutions were prepared. Bacterial cells were again spread on Mueller–Hinton agar plates (placed in a refrigerator for 10 min to stabilize the bacteria on the agar surface) that contain 6 mm size wells. Then, 100 μL of each CeO_2NP sample (1000, 500, 250, 125, and 62.5 $\mu\text{g}/\text{mL}$) was poured in each well, and plates were covered with a parafilm and placed in the incubator at 37 °C for 24 h. The zone of inhibitions was measured using the scale as described in ref 15.

2.4. Antifungal Activities. The antifungal evaluation of CeO_2NPs synthesized through a green approach was

conducted using the agar well inhibition method. To assess the antifungal activity, CeO_2NPs were prepared at concentrations of 62.5, 125, 250, 500, and 1000 $\mu\text{g}/\text{mL}$. Subsequently, 34 g of potato dextrose agar (PDA) was dissolved in 1 L of deionized water. Sterilization of Mueller–Hinton agar was achieved through autoclaving for 3 h at 115 °C using the HICLAVE HVE Model HVE-50 (HIRAYAMA Manufacturing Corp.). Three pathogenic strains of fungi *B. sorokiniana*, *A. flavus*, and *F. oxysporum* were obtained from the mycology laboratory of Pir Mehr Ali Shah Arid Agriculture University, Rawalpindi. The fungal cell suspension was prepared in a PDA broth. The suspension was spread on the agar plates and placed in the refrigerator for 10 min to settle the suspension on the agar surface. The 6 mm wells were made with the help of a cork borer. For negative control, deionized water was used, and the concentrations of positive control fluconazole used against fungal strains were similar to the concentration of CeO_2NPs . The CeO_2NP -treated culture plates were left in an incubator at 37 °C for 3 days. The

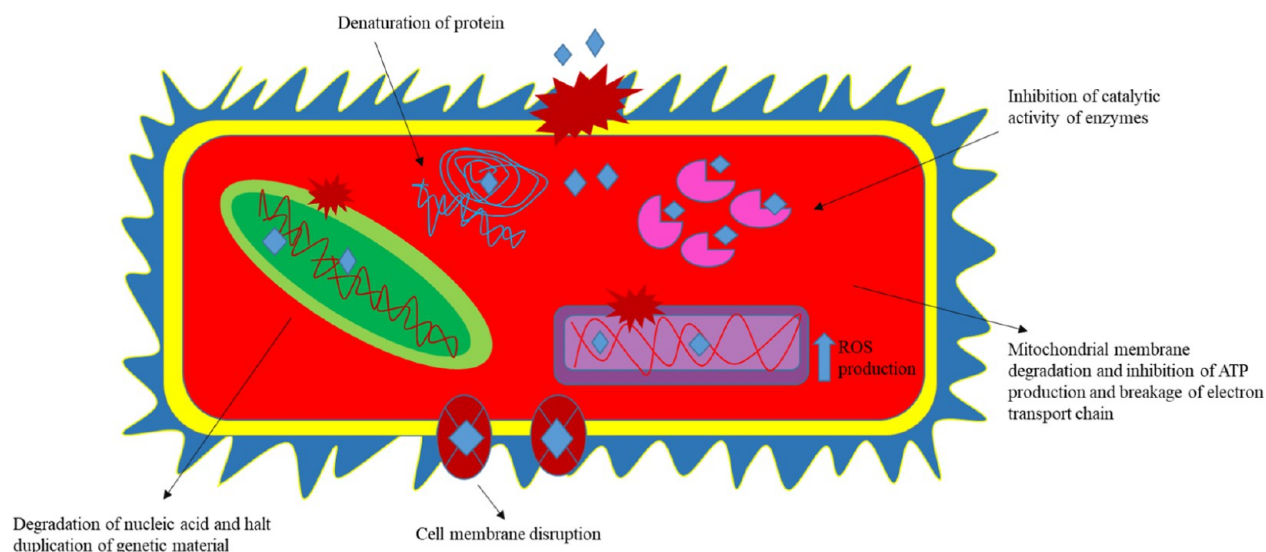


Figure 5. Figurative representation of antibacterial activity of green synthesized CeO₂NPs, chelation at the cell wall induced destabilization and change membrane permeability, and mitochondrial membrane damage causes leakage of ROS. Metal ion chelation with the nuclear membrane inhibit DNA replication, transcription, and translation. Metallic CeO₂NPs cover enzymes' catalytic site and inactivate substrate binding and catalytic activity. The destabilization of membranes imbalances the osmotic potential of bacterial cells and causes cell burst.

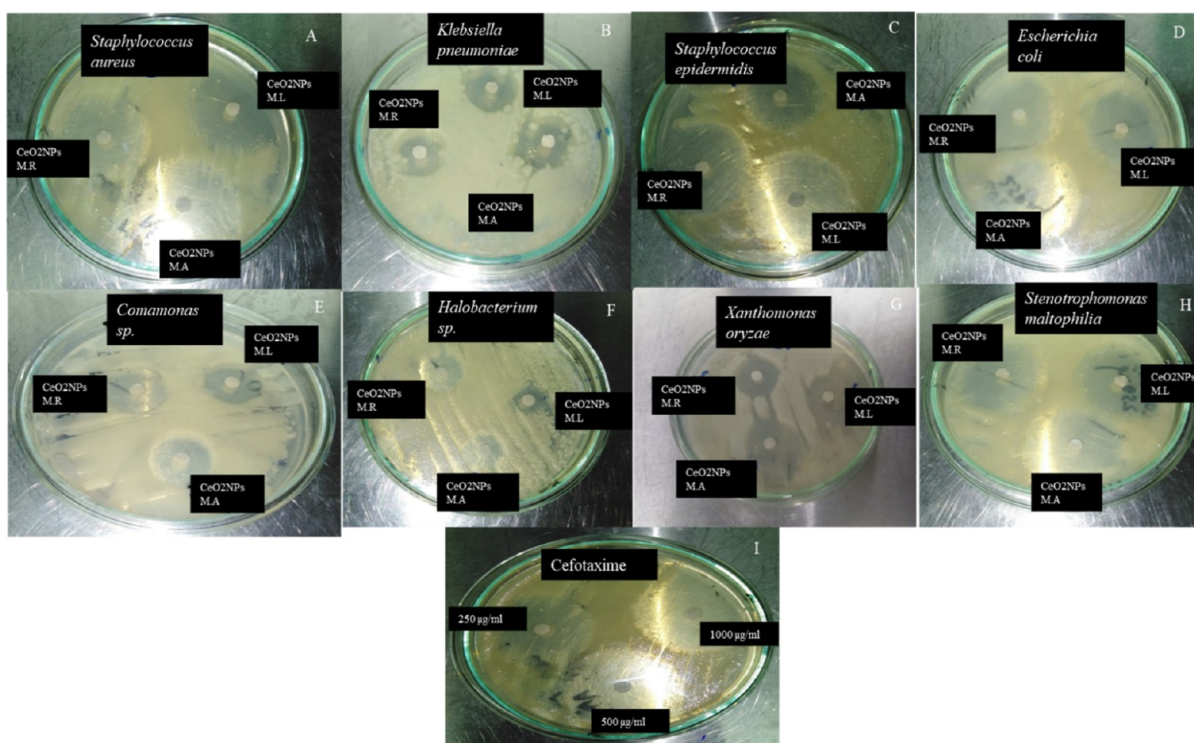


Figure 6. Disc diffusion method was used to explore the antibacterial inhibition potential of CeO₂NPs^{MR}, CeO₂NPs^{ML}, and CeO₂NPs^{MA} and cefotaxime against pathogenic bacterial strains (A) *S. aureus*, (B) *K. pneumoniae*, (C) *S. epidermidis*, (D) *E. coli*, (E) *Comamonas* sp., (F) *Halobacterium* sp., (G) *X. oryzae*, (H) *S. maltophilia*, and (I) Cefotaxime. Figure represents the zone of inhibition for 1000 µg/mL concentration of three different CeO₂NPs and positive control cefotaxime against eight pathogenic bacterial strains.

mentioned concentrations of CeO₂NPs were prepared in deionized water and injected into each well. The zone of inhibitions was measured using the scale described in ref 15.

$$\text{Inhibition percentage} = (I_1 - I_2)/I_1 \times 100 \quad (1)$$

I_1 represents the value for control and I_2 represents the treatment.

3. RESULTS AND DISCUSSION

3.1. Characterization of CeO₂NPs. The UV–visible spectroscopy results confirm the synthesis of CeO₂NPs using the Mentha leaf extract. The UV–visible results of CeO₂NPs^{MA} showed the absorption peak at 320 nm (Figure 2A), CeO₂NPs^{ML} showed the absorption peak at 330 nm (Figure 3A), and CeONPs^{MR} showed the absorption peak at 270 nm (Figure 4A). The results confirm the synthesis of

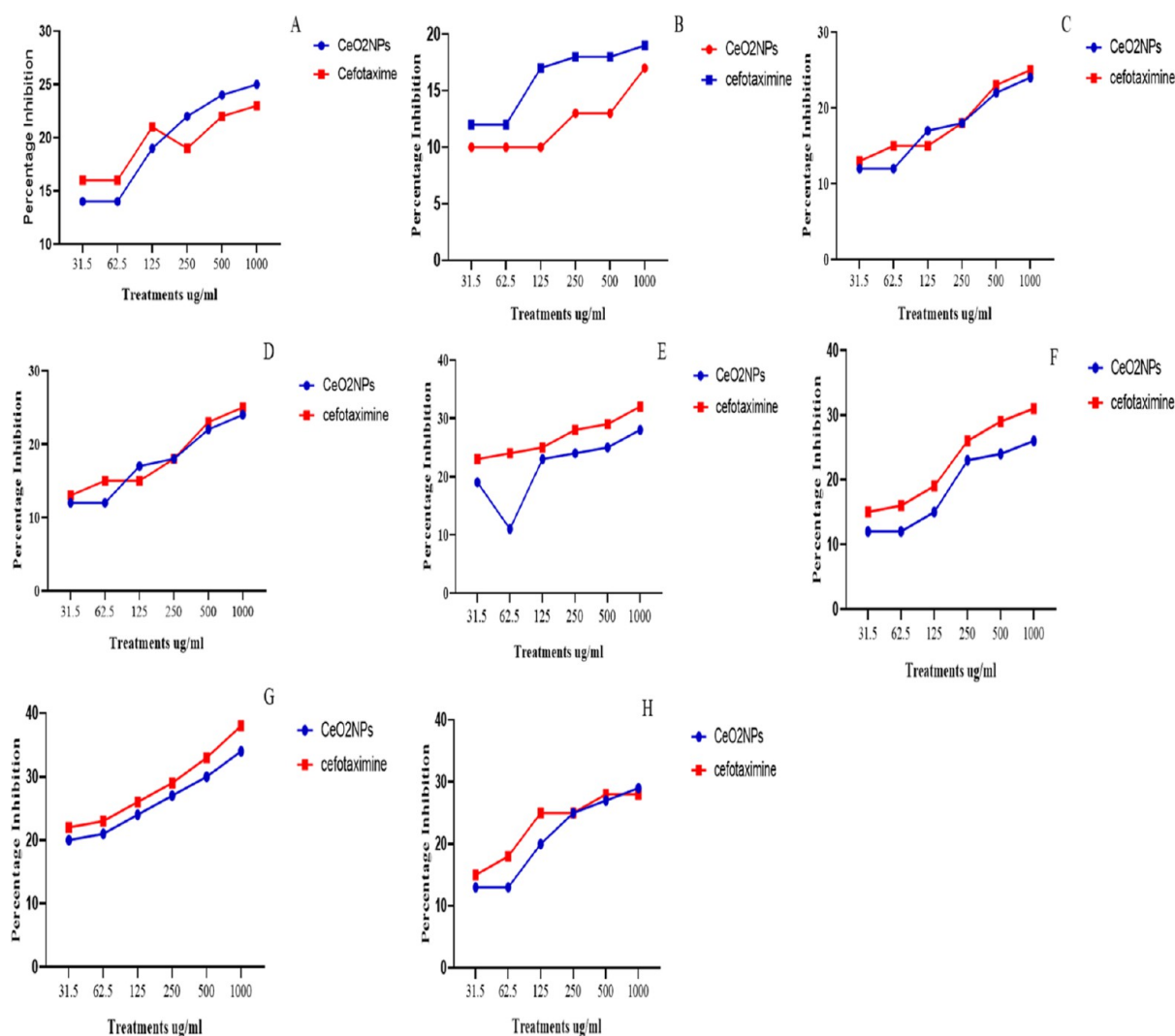


Figure 7. Graphical representation of inhibition potential of CeO₂NPs^{MA} against eight pathogenic bacterial species (A) *S. maltophilia*, (B) *X. oryzae*, (C) *Comamonas* sp., (D) *Halobacterium* sp., (E) *E. coli*, (F) *K. pneumoniae*, (G) *S. aureus*, and (H) *S. epidermidis*.

Table 2. Inhibition Percentage of CeO₂NPs^{MA} against Pathogenic Bacterial Strains

| bacterial species | 31.5 μg/mL | 62.5 μg/mL | 125 μg/mL | 250 μg/mL | 500 μg/mL | 1000 μg/mL |
|--------------------------|--------------|--------------|--------------|--------------|--------------|--------------|
| <i>S. maltophilia</i> | 14.63 ± 0.32 | 14.50 ± 0.50 | 19.50 ± 0.50 | 22.67 ± 0.76 | 24.50 ± 0.50 | 25.50 ± 0.50 |
| <i>X. oryzae</i> | 10.67 ± 0.76 | 10.90 ± 0.85 | 10.60 ± 0.46 | 13.63 ± 0.60 | 13.51 ± 1.57 | 17.40 ± 2.01 |
| <i>Comamonas</i> sp. | 12.47 ± 1.10 | 12.00 ± 0.50 | 17.81 ± 0.58 | 18.50 ± 0.50 | 22.90 ± 0.36 | 24.17 ± 0.58 |
| <i>Halobacterium</i> sp. | 12.17 ± 0.58 | 12.97 ± 0.55 | 17.60 ± 0.61 | 18.61 ± 0.60 | 22.53 ± 1.79 | 24.00 ± 1.11 |
| <i>E. coli</i> | 9.33 ± 0.58 | 11.67 ± 1.04 | 23.67 ± 1.04 | 24.17 ± 0.76 | 25.67 ± 0.76 | 28.23 ± 0.25 |
| <i>K. pneumoniae</i> | 12.07 ± 0.51 | 12.50 ± 0.50 | 15.90 ± 0.36 | 23.57 ± 1.21 | 24.23 ± 0.51 | 26.08 ± 0.25 |
| <i>S. aureus</i> | 20.68 ± 0.76 | 21.08 ± 0.58 | 24.57 ± 0.40 | 27.73 ± 1.08 | 30.30 ± 0.85 | 34.07 ± 0.75 |
| <i>S. epidermidis</i> | 13.54 ± 0.50 | 13.83 ± 0.58 | 20.40 ± 0.85 | 25.57 ± 0.60 | 27.37 ± 0.81 | 29.32 ± 0.33 |

CeO₂NPs. High peak numbers represent the large amount of CeO₂NP synthesis. The size and shape of CeO₂NPs are critical for medicinal use since size and shape are important parameters for absorption of CeO₂NPs into living cells. The size less than 100 nm facilitates the absorption of CeO₂NPs in the cells. The mean size range for CeO₂NPs^{MA} is 34.23–59.34 nm (Figure 2B), CeO₂NPs^{ML} 46.26–80.56 nm (Figure 3B), and CeO₂NPs^{MR} 46.90–55.03 nm (Figure 4B). The spherical shape was observed for all the three green synthesized CeO₂NPs. For Fourier transform infrared spectroscopy, 4000–400 cm⁻¹ spectrum range was used. High

peaks represent highly involved groups like CeO₂NPs^{MA}. The alkyl–aryl–ether and less-involved group was the halo group/amine group (Figure 2D), the CeO₂NPs^{ML} highly involved group was alpha–beta-unsaturated ketone and the less-involved group was the halo group/amine group (Figure 3D), and the CeO₂NPs^{MR} highly involved group was phenol and the less involve group was the halo group/amine group (Figure 4D). The energy-dispersive X-rays used to confirm the elemental composition of a chemical are shown in Figures 2F, 3F, and 4F. Dynamic light scattering spectroscopy was utilized to examine the homogeneity and suspension of CeO₂NPs in

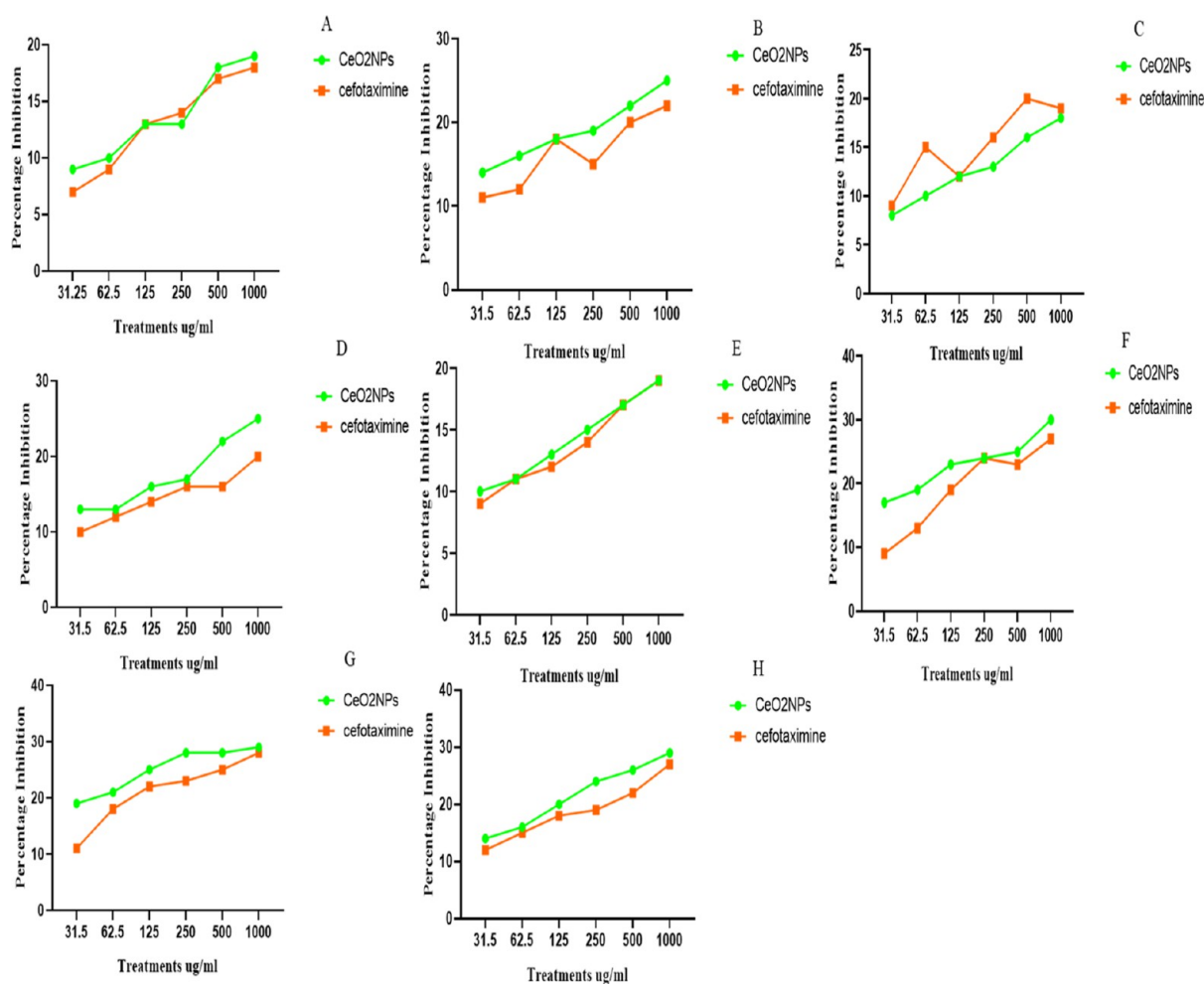


Figure 8. Graphical representation of inhibition potential of $\text{CeO}_2\text{NPs}^{\text{ML}}$ against eight pathogenic bacterial species (A) *E. coli*, (B) *K. pneumoniae*, (C) *Halobacterium* sp., (D) *Comamonas* sp., (E) *X. oryzae*, (F) *S. maltophilia*, (G) *S. aureus*, and (H) *S. epidermidis*.

Table 3. Inhibition Percentage of $\text{CeO}_2\text{NPs}^{\text{ML}}$ against Pathogenic Bacterial Strains

| bacterial species | 31.5 $\mu\text{g/mL}$ | 62.5 $\mu\text{g/mL}$ | 125 $\mu\text{g/mL}$ | 250 $\mu\text{g/mL}$ | 500 $\mu\text{g/mL}$ | 1000 $\mu\text{g/mL}$ |
|--------------------------|-----------------------|-----------------------|----------------------|----------------------|----------------------|-----------------------|
| <i>S. maltophilia</i> | 17.16 \pm 1.04 | 19.56 \pm 0.81 | 23 \pm 0.87 | 24.6 \pm 0.68 | 25.74 \pm 1.72 | 30.1 \pm 1.52 |
| <i>X. oryzae</i> | 10.44 \pm 0.71 | 11.97 \pm 0.45 | 13.1 \pm 0.36 | 15.27 \pm 1.12 | 17.3 \pm 0.79 | 19.93 \pm 0.64 |
| <i>Comamonas</i> sp. | 13.34 \pm 2.41 | 13.16 \pm 2.51 | 16.16 \pm 1.04 | 17.43 \pm 1.91 | 22.72 \pm 0.72 | 25.84 \pm 0.28 |
| <i>Halobacterium</i> sp. | 8.97 \pm 0.49 | 10.84 \pm 0.28 | 12.34 \pm 0.76 | 13.74 \pm 1.86 | 16.24 \pm 1.73 | 18.84 \pm 0.28 |
| <i>E. coli</i> | 9.33 \pm 0.28 | 10.9 \pm 0.36 | 13.00 \pm 0.51 | 13.84 \pm 0.58 | 18.84 \pm 0.77 | 19.57 \pm 0.61 |
| <i>K. pneumoniae</i> | 14.67 \pm 0.29 | 16.34 \pm 0.77 | 18.57 \pm 0.41 | 19.84 \pm 0.28 | 22.9 \pm 0.36 | 25.67 \pm 0.28 |
| <i>S. aureus</i> | 19.67 \pm 0.76 | 21.34 \pm 2.02 | 25.34 \pm 0.28 | 28.34 \pm 0.29 | 28.00 \pm 0.5 | 29.5 \pm 0.5 |
| <i>S. epidermidis</i> | 14.64 \pm 1.07 | 16.47 \pm 0.77 | 20.61 \pm 1.12 | 24.67 \pm 1.04 | 26.17 \pm 1.16 | 29.00 \pm 0.5 |

solution. For pharmaceutical uses, the homogeneity of CeO_2NPs in solution is necessary for the equal entrance of drug into the cell. The polydispersity (PDI) value for $\text{CeO}_2\text{NPs}^{\text{ML}}$ is 0.4 (Figure 3E), that for $\text{CeO}_2\text{NPs}^{\text{MR}}$ is 0.2 (Figure 4E), and that for $\text{CeO}_2\text{NPs}^{\text{MA}}$ is 0.3 (Figure 2E). PDI value less than 0.7 is considered good for pharmaceutical activity. Zeta potential was used to evaluate the net charge on CeO_2NP surface. For $\text{CeO}_2\text{NPs}^{\text{ML}}$, the electromobility value was -3.117 mV (Figure 3G), for $\text{CeO}_2\text{NPs}^{\text{MA}}$, the electromobility value was -2.141 mv (Figure 2G), and for $\text{CeO}_2\text{NPs}^{\text{MR}}$, the electromobility value was -3.293 mV (Figure 4G). The positive charge was observed on all the three CeO_2NP surfaces. Atomic force microscopy, an advanced technique, diagnoses the size of CeO_2NPs below

30 nm. The size for $\text{CeO}_2\text{NPs}^{\text{MA}}$ is 4.5–9.1 nm (Figure 2C), that for $\text{CeO}_2\text{NPs}^{\text{MR}}$ is 10 nm (Figure 4C), and that for $\text{CeO}_2\text{NPs}^{\text{ML}}$ is 3.5–5 nm (Figure 3C) (see Table 1).

3.2. Antibacterial Activity of CeO_2NPs against Bacterial Pathogens. The interaction of CeO_2NPs with bacterial cells is the most essential phenomenon to study. The positively charged surface of CeO_2NPs facilitates the bond formation with the lipid bilayer of membranes. The oxidation of a selectively permeable membrane due to CeO_2NPs induced imbalance in the cellular osmotic potential. CeO_2NPs have a significant negative effect on bacterial cells, primarily affecting the bacterial cell membrane and disrupting the plasma membrane. Furthermore, CeO_2NPs promote mitophagy, resulting in an increased production of ROS. This

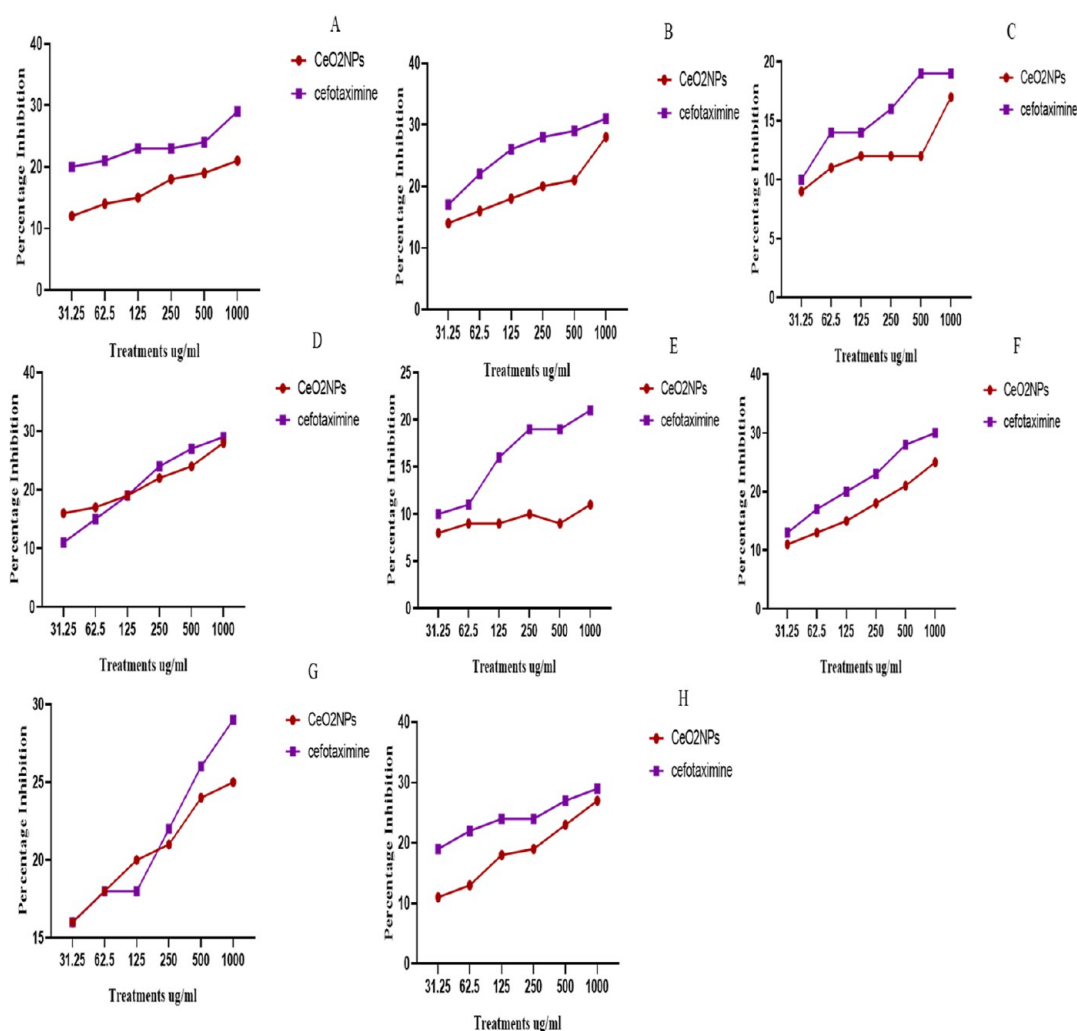


Figure 9. Graphical representation of inhibition potential of $\text{CeO}_2\text{NPs}^{\text{M,R}}$ against eight pathogenic bacterial species (A) *E. coli*, (B) *K. pneumoniae*, (C) *Halobacterium* sp., (D) *Comamonas* sp., (E) *X. oryzae*, (F) *S. maltophilia*, (G) *S. aureus*, and (H) *S. epidermidis*.

Table 4. Inhibition Percentage of $\text{CeO}_2\text{NPs}^{\text{M,R}}$ against Pathogenic Bacterial Strains

| bacterial species | 31.5 $\mu\text{g/mL}$ | 62.5 $\mu\text{g/mL}$ | 125 $\mu\text{g/mL}$ | 250 $\mu\text{g/mL}$ | 500 $\mu\text{g/mL}$ | 1000 $\mu\text{g/mL}$ |
|-------------------------|-----------------------|-----------------------|----------------------|----------------------|----------------------|-----------------------|
| <i>S. maltophilia</i> | 11.84 \pm 0.29 | 13.34 \pm 0.29 | 15.17 \pm 0.28 | 18.84 \pm 0.28 | 21.84 \pm 1.26 | 25.5 \pm 0.5 |
| <i>X. oryzae</i> | 8.34 \pm 0.28 | 9.00 \pm 0.5 | 9.5 \pm 0.5 | 10.34 \pm 1.61 | 9.34 \pm 1.04 | 11.00 \pm 0.5 |
| <i>Comamonas</i> sp. | 16.67 \pm 0.55 | 17.97 \pm 0.42 | 19.74 \pm 0.35 | 22.3 \pm 0.85 | 24.86 \pm 0.58 | 28.74 \pm 0.46 |
| <i>Halobacterium</i> sp | 9.5 \pm 0.5 | 11.00 \pm 0.5 | 12.17 \pm 0.58 | 12.5 \pm 1.38 | 12.67 \pm 0.28 | 17.5 \pm 0.5 |
| <i>E. coli</i> | 12.07 \pm 0.56 | 14.67 \pm 0.28 | 15.24 \pm 0.25 | 18.57 \pm 0.41 | 19.74 \pm 0.69 | 21.24 \pm 1.51 |
| <i>K. pneumoniae</i> | 14.24 \pm 0.25 | 16.84 \pm 1.27 | 18.57 \pm 0.41 | 20.34 \pm 1.06 | 21.74 \pm 1.07 | 28.67 \pm 0.38 |
| <i>S. aureus</i> | 16.5 \pm 0.5 | 18.34 \pm 0.29 | 20.67 \pm 1.05 | 21.74 \pm 0.47 | 24.4 \pm 0.53 | 25.84 \pm 0.29 |
| <i>S. epidermidis</i> | 11.74 \pm 0.69 | 13.00 \pm 0.5 | 18.17 \pm 0.77 | 19.17 \pm 0.58 | 23.74 \pm 0.41 | 27.84 \pm 0.76 |

increased oxidative stress contributes to intracellular destruction, resulting in protein denaturation, DNA strand fragmentation, and cell cycle arrest. CeO_2NPs ' multifaceted impact highlights their potential as agents for causing extensive damage to bacterial structures and functions (Figure 5). The antimicrobial capacity of CeO_2NPs toward Gram-negative and Gram-positive bacteria was explored using the agar well diffusion method. The zone of inhibition was measured against all pathogens. However, the results revealed that CeO_2NPs 1000 $\mu\text{g/mL}$ possessed effective antibacterial activity against Gram-positive *S. aureus* (Figure 6A) and *S. epidermidis* (Figure 6C), and CeO_2NPs were less virulent against Gram-negative *E. coli* (Figure 6D), *S. maltophilia*

(Figure 6H), *Comamonas* sp. (Figure 6E), *Halobacterium* sp. (Figure 6F), and *K. pneumoniae* (Figure 6B) and plant bacterial *Xanthomonas* sp. (Figure 6G) and Cefotaxime (Figure 6I). The $\text{CeO}_2\text{NPs}^{\text{M,A}}$ at 1000 $\mu\text{g/mL}$ concentration, maximum inhibition zone 25.50 \pm 0.50 mm against *S. maltophilia* (Figure 7A and Table 2), 17.40 \pm 2.01 mm against *X. oryzae* (Figure 7B and Table 2), 24.17 \pm 0.58 mm against *Comamonas* sp. (Figure 7C and Table 2), 24.00 \pm 1.00 mm against *Halobacterium* sp. (Figure 7D and Table 2), 28.23 \pm 0.25 mm against *E. coli* (Figure 7E and Table 2), and 26.08 \pm 0.51 mm against *K. pneumoniae* (Figure 7F and Table 2), whereas 34.07 \pm 0.75 mm against *S. aureus* (Figure 7G and Table 2) and 29.32 \pm 0.33 mm against *S. epidermidis* (Figure

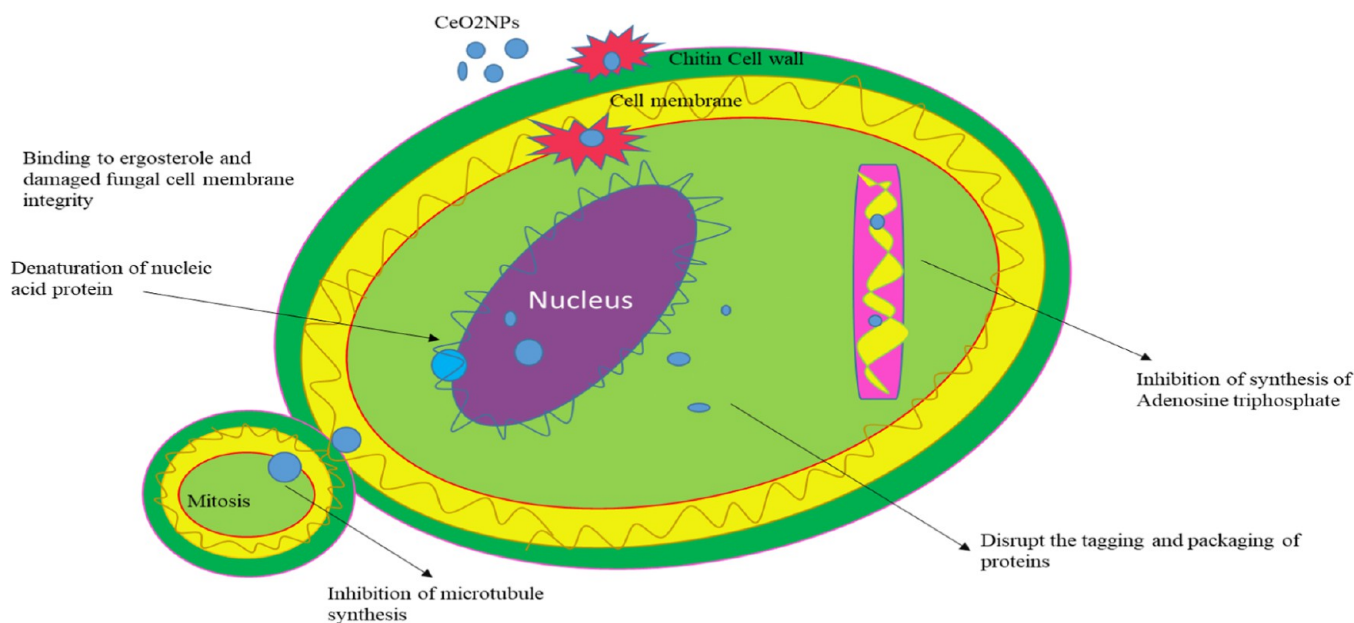


Figure 10. Figurative representation of antifungal activity of green synthesized CeO₂NP-induced apoptosis through ROS generation against fungal cell. Intracellular destruction accelerates disruption of nucleus and nucleic acids and chelation of metallic CeO₂NPs at mitochondrial membrane induce disruption of ETC and ATP production and destabilization of cellular homeostasis.

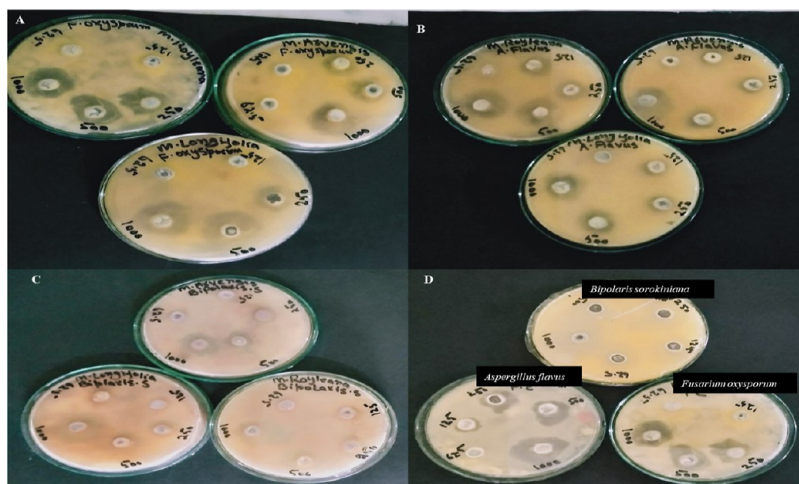


Figure 11. Agar well plate method was used to evaluate the antifungal inhibition potential of CeO₂NPs^{MR}, CeO₂NPs^{ML}, and CeO₂NPs^{MA} and fluconazole against pathogenic fungal species (A) *F. oxysporum*, (B) *A. flavus*, (C) *B. sorokiniana*, and (D) Fluconazole. Activity was checked for (62.5, 125, 250, 500, and 1000 µg/mL) of three different CeO₂NPs and positive control was Fluconazole.

7H and Table 2). However, the antibacterial activity of CeO₂NPs^{ML} showed efficient killing potential at 1000 µg/mL and a maximal inhibition zone of 19.57 ± 0.61 mm against *E. coli* (Figure 8A and Table 3), 25.67 ± 0.28 mm against *K. pneumoniae* (Figure 8B and Table 3), 18.83 ± 0.28 mm against *Halobacterium* sp. (Figure 8C and Table 3), 25.83 ± 0.28 mm against *Comamonas* sp. (Figure 8D and Table 3), 19.93 ± 0.65 mm against *Xanthomonas* sp. (Figure 8E and Table 3), 30.1 ± 1.59 mm against *S. maltophilia* (Figure 8F and Table 3), 29.5 ± 0.5 mm against *S. aureus* (Figure 8G and Table 3), and 29.00 ± 0.5 mm against *S. epidermidis* (Figure 8H and Table 3). However, the antibacterial activity of CeO₂NPs^{MR} exhibits satisfactory killing potential at 1000 µg/mL, and the maximal inhibition zone is 21.23 ± 1.51 mm against *E. coli* (Figure 9A and Table 4), 28.67 ± 0.37 mm against *K. pneumoniae* (Figure 9B and Table 4), 17.50 ± 0.50

mm against *Halobacterium* sp. (Figure 9C and Table 4), 28.73 ± 0.40 mm against *Comamonas* sp. (Figure 9D and Table 4), 11.50 ± 0.5 mm against *Xanthomonas* sp. (Figure 9E and Table 4), 25.5 ± 0.5 mm against *S. maltophilia* (Figure 9F and Table 4), 25.83 ± 0.28 mm against *S. aureus* (Figure 9G and Table 4), and 27.83 ± 0.76 mm against *S. epidermidis* (Figure 9H and Table 4). The antibacterial efficiency of CeO₂NPs tested against *S. aureus*, *S. epidermidis*, *E. coli*, *S. maltophilia*, *Comamonas* sp., *Halobacterium* sp., *K. pneumoniae*, *Xanthomonas* sp., and cytotoxicity was statistically significant for all the three CeO₂NPs. CeO₂NPs showed maximum inhibition potential due to small size, allowing rapid absorption in bacterial cells compared with the bulk material. CeO₂NPs' antibacterial mechanism involves direct interaction with the bacterial cell and induce production of secondary toxic substances that can lead to detrimental/septic effects and

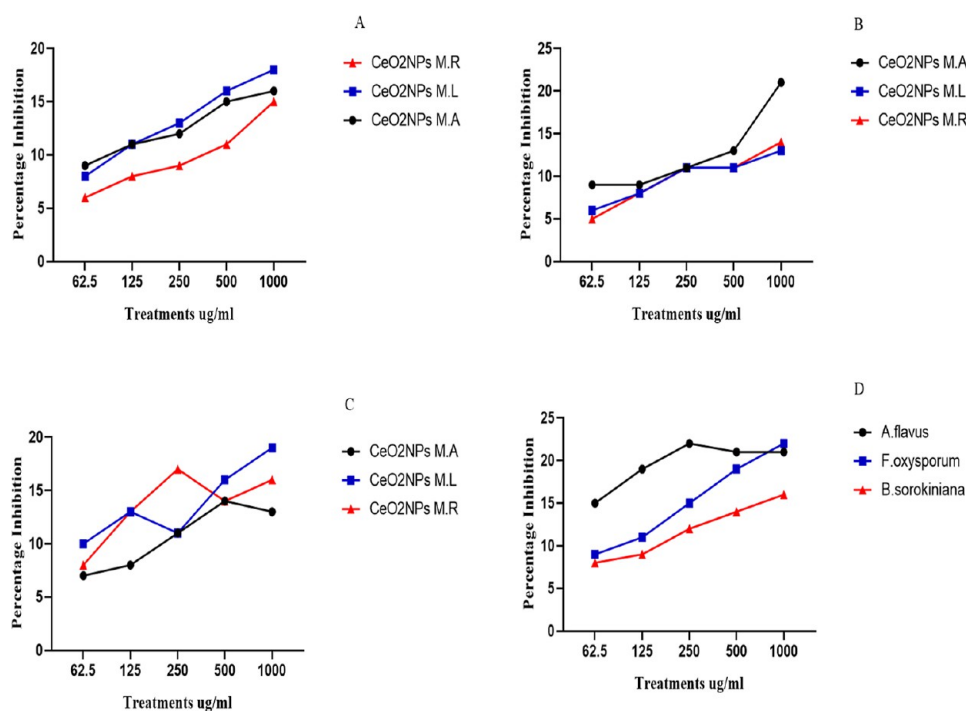


Figure 12. Graphical representation of inhibition percentage of CeO₂NPs^{M,R}, CeO₂NPs^{M,L}, and CeO₂NPs^{M,A} and fluconazole against pathogenic fungal species (A) *A. flavus*, (B) *F. oxysporum*, (C) *B. sorokiniana*, and (D) Fluconazole.

resultant cell death.¹⁶ Previous research data presented that CeO₂NPs showed effective bactericidal potential due to ROS liberation ROS by causing mitophagy and degradation inside the mitochondrial membrane, breakage of electron transport chain (ETC), and leakage of free radical species which induce further oxidation of other subcellular organelles.^{16,17} The data of antibacterial activity revealed that CeO₂NPs are highly toxic against Gram-positive and Gram-negative bacterial species. CeO₂NPs stimulate oxidation of peptidoglycan and lipid peroxidation of the cell membrane resulting in leakage of the cellular material.

3.3. Antifungal Activity of CeO₂NPs. CeO₂NPs' inhibitory effects on three fungal species, *A. flavus* (Figure 11B), *F. oxysporum* (Figure 11A), and *B. sorokiniana* (Figure 11C), Fluconazole (Figure 11D), were investigated. The antifungal activity of CeO₂NPs at five different concentrations was determined by using the agar well diffusion method on PDA. The efficient growth inhibition was caused by CeO₂NPs. *A. flavus*, *F. oxysporum*, and *B. sorokiniana* are plant pathogenic fungal species that destroyed many cereal crops every year worldwide (Figure 10). *B. sorokiniana* is one of the popular wheat pathogens attacking all parts of the wheat including shoot, seed, root, and leaves. Spot blotch, root rot, crown rot, and black point are diseases caused by *B. sorokiniana* in wheat.¹⁸ *F. oxysporum* belongs to group ascomycota and causes disease in *Solanaceae* crops and weeds like crabgrass, pigweed, and mallow. *F. oxysporum* induced vascular wilt disease, penetrates in rootlets, and mostly colonized in xylem vessels of plants and particularly infect herbaceous plants and large woody trees especially in tropical and temperate regions.¹⁹ *A. flavus* is a saprotrophic, pathogenic fungus and is distributed worldwide. *A. flavus* species produces aflatoxins, the highly poisonous hepatocarcinogenic natural compounds ever isolated and characterized. *A. flavus* particularly colonized cereal crop grains and constantly

infected next generations. The fungal spores are poisonous to both humans and animals; even ingestion of fungal infected seeds cause death of animals and severe respiratory and cutaneous allergy in humans.²⁰

For *B. sorokiniana*, the maximum inhibitory potential of three different green synthesized CeO₂NPs and zone of inhibition at 1000 μg/mL were CeO₂NPs^{M,A} 13.7 ± 1.81, CeO₂NPs^{M,L} 19.7 ± 1.54, and CeO₂NPs^{M,R} 16.28 ± 0.99 (Figure 12C and Table 5). For *A. flavus*, the maximum inhibitory potential of three different green synthesized CeO₂NPs and zone of inhibition at 1000 μg/mL was CeO₂NPs^{M,A} 13.1 ± 0.33, CeO₂NPs^{M,L} 13.57 ± 0.47, and CeO₂NPs^{M,R} 12.54 ± 0.35 (Figure 12A and Table 5). For *F. oxysporum* maximum inhibitory potential of three different green synthesized CeO₂NPs and zone of inhibition at 1000 μg/mL was CeO₂NPs^{M,A} 21.97 ± 0.41, CeO₂NPs^{M,L} 13.4 ± 0.17, and CeO₂NPs^{M,R} 14.67 ± 0.52 (Figure 12B and Table 5). For positive control fluconazole, the maximum inhibitory potential of three different green synthesized CeO₂NPs and zone of inhibition at 1000 μg/mL was *B. sorokiniana* 16.64 ± 0.42, *F. oxysporum* 22.5 ± 0.57, and *A. flavus* 21.974 ± 0.29 (Figure 12D and Table 5).

The present research study revealed that the green synthesized CeO₂NPs imposed significant antifungal effects against plant pathogens. The popular antifungal drug fluconazole was used as a positive control in the given study. The electropositive surface charge of CeO₂NPs is supportive to interact with hyphae and due to small-size CeO₂NPs cross the chitin cell wall, penetrate in fungal cells, and alter fungal cell metabolism. Green synthesized CeO₂NPs have high surface-to-volume ratio and were known for their excellent antifungal activities and better moieties to contact with the cell membrane and also detrimental for chitin cell wall.²¹ CeO₂NPs efficiently contact with sulfur- and phosphorus-containing components of a cell. Sulfur is the

Table S. Inhibition Percentage of CeO₂NPs against Pathogenic Fungi

| concentrations ($\mu\text{g}/\text{mL}$) | A. flavus | | | F. oxysporum | | | B. sorokiniana | | |
|--|-------------------------------------|-------------------------------------|-------------------------------------|-------------------------------------|-------------------------------------|-------------------------------------|-------------------------------------|-------------------------------------|-------------------------------------|
| | CeO ₂ NPs ^{M,L} | CeO ₂ NPs ^{M,A} | CeO ₂ NPs ^{M,R} | CeO ₂ NPs ^{M,L} | CeO ₂ NPs ^{M,A} | CeO ₂ NPs ^{M,R} | CeO ₂ NPs ^{M,L} | CeO ₂ NPs ^{M,A} | CeO ₂ NPs ^{M,R} |
| 62.5 | 8.26 ± 0.25 | 9.00 ± 0.2 | 11.1 ± 0.17 | 6.16 ± 0.05 | 9.06 ± 0.11 | 5.13 ± 0.15 | 10.65 ± 0.66 | 7.23 ± 0.25 | 8.43 ± 0.52 |
| 125 | 11.26 ± 0.37 | 11.23 ± 0.23 | 11.26 ± 0.28 | 8.16 ± 0.05 | 9.26 ± 0.11 | 8.1 ± 0.1 | 13.57 ± 1.01 | 8.1 ± 0.2 | 13.3 ± 1.47 |
| 250 | 11.73 ± 0.40 | 11.8 ± 0.52 | 11.3 ± 0.2 | 11.5 ± 0.26 | 11.66 ± 0.23 | 11.4 ± 0.17 | 11.96 ± 0.25 | 11.43 ± 0.49 | 17.73 ± 1.11 |
| 500 | 12.4 ± 0.72 | 11.9 ± 0.26 | 11.43 ± 0.21 | 11.76 ± 0.51 | 13.26 ± 0.28 | 11.76 ± 0.05 | 16.06 ± 0.62 | 14.83 ± 0.56 | 14.26 ± 1.05 |
| 1000 | 13.56 ± 0.47 | 13.1 ± 0.3 | 12.53 ± 0.35 | 13.4 ± 0.17 | 21.96 ± 0.40 | 14.66 ± 0.51 | 19.66 ± 1.54 | 13.7 ± 1.81 | 16.28 ± 0.99 |

critical part of amino acids, and phosphorus is the building block of DNA, and both are best sites for nanoparticle binding/attachments.²² Another suggested mechanism is that fungi cell walls made up of chitin (a long-chain amino polysaccharide polymer consists of *N*-acetylglucosamine) are hard enough to provide protection to fungicides, but CeO₂NPs due to their nanosize efficiently cross the cell wall through interacting with glucose components and cause breakage and leakage of the cellular material.²³

4. CONCLUSIONS

The research study revealed that the results of the antimicrobial activity of green synthesized CeO₂NPs were efficacious against all selected pathogenic bacterial strains. The antibacterial activity of CeO₂NPs was high against Gram-positive bacterial strains (*S. aureus* and *S. epidermidis*). In the case of Gram-negative bacteria *Halobacterium* sp., *Comamonas* sp., and *X. oryzae*, less inhibitory potential of CeO₂NPs was noticed. For *E. coli*, *K. pneumoniae*, and *S. maltophilia*, the CeO₂NP toxicity was significantly high, and good antibacterial inhibition percentage was observed. The antifungal potential of CeO₂NPs was checked against three plant pathogenic fungal species. The effectual inhibitory potential of green synthesized CeO₂NPs was observed against *A. flavus* and *F. oxysporum*. The less diameter inhibition zones were observed for *B. sorokiniana*. Among all the three different plant-based nanoparticles, CeO₂NPs^{M,L} and CeO₂NPs^{M,A} were significantly toxic against microbial species. The antimicrobial activity of CeO₂NPs^{M,R} was slightly less effective against selected bacterial and fungal species.

Three different *Mentha* species were collected from different cities of Pakistan, and the biotic and abiotic stress level determined the secondary metabolite production and composition in plants. The plant extract used for the reduction of nanoparticles contained a variable proportion of phytochemicals which are pharmaceutically important for the treatment of diseases. The green synthesized CeO₂NPs that possess coating of these phytochemicals play an important role in biological interaction. Unique size-to-volume ratio enhanced CeO₂NP penetration power and easily cross-selective-permeable membranes. The CeO₂NPs induced the oxidation of subcellular organelles and denaturation of proteins DNA and RNA which arrest cell cycle activity and halt bacterial and fungal cell duplication.

■ ASSOCIATED CONTENT

Data Availability Statement

All data generated or analyzed during this study are included in this published article.

■ AUTHOR INFORMATION

Corresponding Authors

Zia-ur-Rehman Mashwani – Department of Botany, Pir Mehr Ali Shah (PMAS)-Arid Agriculture University, Rawalpindi 46000, Pakistan; Pakistan Academy of Sciences, Islamabad 44010, Pakistan; orcid.org/0000-0003-4222-7708; Email: Zia.Botany@gmail.com

Sohail – College of Bioscience and Biotechnology, Yangzhou University, Yangzhou, Jiangsu 225009, China; orcid.org/0000-0002-0349-7214; Email: Sohail.botanist@hotmail.com

Authors

Maarij Khan – Department of Botany, Pir Mehr Ali Shah (PMAS)-Arid Agriculture University, Rawalpindi 46000, Pakistan

Rahmat Wali – Department of Botany, Pir Mehr Ali Shah (PMAS)-Arid Agriculture University, Rawalpindi 46000, Pakistan

Naveed Iqbal Raja – Department of Botany, Pir Mehr Ali Shah (PMAS)-Arid Agriculture University, Rawalpindi 46000, Pakistan

Riaz Ullah – Department of Pharmacognosy, College of Pharmacy King Saud University, Riyadh 11451, Saudi Arabia; orcid.org/0000-0002-2860-467X

Ahmed Bari – Department of Pharmaceutical Chemistry, College of Pharmacy King Saud University, Riyadh 11451, Saudi Arabia

Shah Zaman – Department of Botany, University of Malakand KPK, Chakdara 18800, Pakistan

Complete contact information is available at:

<https://pubs.acs.org/10.1021/acsomega.4c00236>

Author Contributions

M.K., Z.-u.-R.M., and S. conceived the idea; M.K., Z.-u.-R.M., and S. performed the experiment; M.K., Z.-u.-R.M., R.w., and N.I.R. collected, analyzed, and interpreted the data; M.K. and S. wrote the manuscript and shared the first draft; R.U. and A.B. contributed to funding acquisition; and S.Z. and S. reviewed the final version of the article. All authors read and approved the final manuscript.

Notes

The authors declare no competing financial interest.

ACKNOWLEDGMENTS

The authors wish to thank Researchers Supporting Project number (RSP2024R346) at King Saud University, Riyadh, Saudi Arabia for financial support.

REFERENCES

- (1) Prestinaci, F.; Pezzotti, P.; Pantosti, A. Antimicrobial resistance: a global multifaceted phenomenon. *Pathog. Global Health* **2015**, *109* (7), 309–318.
- (2) Rice, L. B. Federal funding for the study of antimicrobial resistance in nosocomial pathogens: no ESKAPE. *J. Infect. Dis.* **2008**, *197* (8), 1079–1081.
- (3) Mulani, M. S.; Kamble, E. E.; Kumkar, S. N.; Tawre, M. S.; Pardesi, K. R. Emerging strategies to combat ESKAPE pathogens in the era of antimicrobial resistance: a review. *Front. Microbiol.* **2019**, *10*, 539.
- (4) Santaniello, A.; Sansone, M.; Fioretti, A.; Menna, L. F. Systematic review and meta-analysis of the occurrence of ESKAPE bacteria group in dogs, and the related zoonotic risk in animal-assisted therapy, and in animal-assisted activity in the health context. *Int. J. Environ. Res. Public Health* **2020**, *17* (9), 3278.
- (5) Read, A. F.; Woods, R. J. Antibiotic resistance management. *Evol. Med. Public Health.* **2014**, *2014* (1), 147.
- (6) Kamaruzzaman, N. F.; Tan, L. P.; Hamdan, R. H.; Choong, S. S.; Wong, W. K.; Gibson, A. J.; Chivu, A.; Pina, M. d. F. Antimicrobial polymers: the potential replacement of existing antibiotics? *Int. J. Mol. Sci.* **2019**, *20* (11), 2747.
- (7) Mohr, A.; Simon, M.; Joha, T.; Hanses, F.; Salzberger, B.; Hitzentbichler, F. Epidemiology of candidemia and impact of infectious disease consultation on survival and care. *Infection* **2020**, *48*, 275–284.
- (8) Zhang, L.; Zhou, S.; Pan, A.; Li, J.; Liu, B. Surveillance of antifungal susceptibilities in clinical isolates of *Candida* species at 36

hospitals in China from 2009 to 2013. *Int. J. Infect. Dis.* **2015**, *33*, 1–4.

(9) Gambardella, C.; Mesarič, T.; Milivojević, T.; Sepčić, K.; Gallus, L.; Carbone, S.; Ferrando, S.; Faimali, M. Effects of selected metal oxide nanoparticles on *Artemia salina* larvae: evaluation of mortality and behavioural and biochemical responses. *Environ. Monit. Assess.* **2014**, *186*, 4249–4259.

(10) Goharshadi, E. K.; Samiee, S.; Nancarrow, P. Fabrication of cerium oxide nanoparticles: Characterization and optical properties. *J. Colloid Interface Sci.* **2011**, *356* (2), 473–480.

(11) Khan, M.; Sohail; Raja, N. I.; Asad, M. J.; Mashwani, Z. U. R. Antioxidant and hypoglycemic potential of phytochemical cerium oxide nanoparticles. *Sci. Rep.* **2023**, *13* (1), 4514.

(12) Thakur, N.; Manna, P.; Das, J. Synthesis and biomedical applications of nanoceria, a redox active nanoparticle. *J. Nanobiotechnol.* **2019**, *17* (1), 84.

(13) Pop, O. L.; Mesaros, A.; Vodnar, D. C.; Suharoschi, R.; Tăbăran, F.; Mageruşan, L.; Tóodor, I. S.; Diaconeasa, Z.; Balint, A.; Ciontea, L.; et al. Cerium oxide nanoparticles and their efficient antibacterial application in vitro against gram-positive and gram-negative pathogens. *Nanomaterials* **2020**, *10* (8), 1614.

(14) Dar, M. A.; Gul, R.; Alfadda, A. A.; Karim, M. R.; Kim, D. W.; Cheung, C. L.; Almajid, A. A.; Alharthi, N. H.; Pulakat, L. Size-dependent effect of nanoceria on their antibacterial activity towards *Escherichia coli*. *Sci. Adv. Mater.* **2017**, *9* (7), 1248–1253.

(15) Zahara, K.; Bibi, Y.; Qayyum, A.; Nisa, S. Investigation of antimicrobial and antioxidant properties of *Bidens Biternata*. *Iran. J. Sci. Technol. Trans. A: Sci.* **2019**, *43*, 725–734.

(16) Zhang, M.; Zhang, C.; Zhai, X.; Luo, F.; Du, Y.; Yan, C. Antibacterial mechanism and activity of cerium oxide nanoparticles. *Sci. China Mater.* **2019**, *62* (11), 1727–1739.

(17) Farias, I. A. P.; Santos, C. C. L. D.; Sampaio, F. C. Antimicrobial activity of cerium oxide nanoparticles on opportunistic microorganisms: a systematic review. *BioMed Res. Int.* **2018**, *2018*, 1923606.

(18) Al-Sadi, A. M. Bipolaris sorokiniana-induced black point, common root rot, and spot blotch diseases of wheat: A review. *Front. Cell. Infect. Microbiol.* **2021**, *11*, 584899.

(19) Michielse, C. B.; Rep, M. Pathogen profile update: *Fusarium oxysporum*. *Mol. Plant Pathol.* **2009**, *10* (3), 311–324.

(20) Hedayati, M. T.; Pasqualotto, A. C.; Warn, P. A.; Bowyer, P.; Denning, D. W. *Aspergillus flavus*: human pathogen, allergen and mycotoxin producer. *Microbiology* **2007**, *153* (6), 1677–1692.

(21) Devi, N. S.; Ganapathy, D. M.; Rajeshkumar, S.; Maiti, S. Characterization and antimicrobial activity of cerium oxide nanoparticles synthesized using neem and ginger. *J. Adv. Pharm. Technol. Res.* **2022**, *13* (Suppl 2), S491.

(22) Rahdar, A.; Beyzaei, H.; Askari, F.; Kyzas, G. Z. Gum-based cerium oxide nanoparticles for antimicrobial assay. *Appl. Phys. A: Mater. Sci. Process.* **2020**, *126*, 324.

(23) Eka Putri, G.; Rilda, Y.; Syukri, S.; Labanni, A.; Arief, S. Highly antimicrobial activity of cerium oxide nanoparticles synthesized using *Moringa oleifera* leaf extract by a rapid green precipitation method. *J. Mater. Res. Technol.* **2021**, *15*, 2355–2364.

(24) Tafarihi, M.; Imran, M.; Tufail, T.; Gondal, T. A.; Caruso, G.; Sharma, S.; Sharma, R.; Atanassova, M.; Atanassov, L.; Valere Tsouh Fokou, P.; et al. The wonderful activities of the genus *Mentha*: Not only antioxidant properties. *Molecules* **2021**, *26* (4), 1118.

(25) Jakupec, M. A.; Unfried, P.; Keppler, B. K. Pharmacological properties of cerium compounds. *Rev. Physiol., Biochem. Pharmacol.* **2005**, *153*, 101–111.

(26) Khan, M.; Mashwani, Z. U. R.; Ikram, M.; Raja, N. I.; Mohamed, A. H.; Ren, G.; Omar, A. A. Efficacy of green cerium oxide nanoparticles for potential therapeutic applications: Circumstantial insight on mechanistic aspects. *Nanomaterials* **2022**, *12* (12), 2117.

(27) Faisal, S.; Jan, H.; Shah, S. A.; Shah, S.; Khan, A.; Akbar, M. T.; Rizwan, M.; Jan, F.; Wajidullah; Akhtar, N.; et al. Green synthesis of zinc oxide (ZnO) nanoparticles using aqueous fruit extracts of

Myristica fragrans: their characterizations and biological and environmental applications. *ACS Omega* **2021**, *6* (14), 9709–9722.

(28) Brahmi, F.; Khodir, M.; Mohamed, C.; Pierre, D. Chemical composition and biological activities of Mentha species. *Aromatic and medicinal Plants-Back to Nature*; InTech, 2017; Vol. 10, pp 47–79.

(29) Zhou, F.; Peterson, T.; Fan, Z.; Wang, S. The Commonly Used Stabilizers for Phytochemical-Based Nanoparticles: Stabilization Effects, Mechanisms, and Applications. *Nutrients* **2023**, *15* (18), 3881.